Sequential Damage Detection based on the Continuous Wavelet Transform

Yizheng Liao[a] and Konstantinos Balafas[b] and Ram Rajagopal[a] and Anne S. Kiremidjian[b]

[a]Stanford Sustainable Systems Lab, Department of Civil and Environmental Engineering, Stanford University, 473 Via Ortega, Stanford, CA United States;
[b]Department of Civil and Environmental Engineering, Stanford University, 473 Via Ortega, Stanford, CA United States

ABSTRACT

This paper presents a sequential structural damage detection algorithm that is based on a statistical model for the wavelet transform of the structural responses. The detector uses the coefficients of the wavelet model and does not require prior knowledge of the structural properties. Principal Component Analysis is applied to select and extract the most sensitive features from the wavelet coefficients as the damage sensitive features. The damage detection algorithm is validated using the simulation data collected from a four-story steel moment frame. Various features have been explored and the detection algorithm was able to identify damage. Additionally, we show that for a desired probability of false alarm, the proposed detector is asymptotically optimal on the expected delay.

Keywords: Earthquake Damage Detection, Continuous Wavelet Transform, Bayesian Detection, Sequential Detection, Structural Health Monitoring

1. INTRODUCTION

The application of Statistical Pattern Recognition (SPR) in the field of Structural Health Monitoring (SHM) has received significant attention by researchers over the past few decades, especially in the area of vibration analysis of structures. There has been considerable research in the application of various pattern recognition methods for damage detection[1–3] while a more formal presentation of the Statistical Pattern Recognition Paradigm can be found in Refs. 4 and 5. In SPR, damage is detected through changes or outliers in statistical features that are obtained directly from the acquired data rather than by changes in estimates of structural properties. As a result, one of the advantages of SPR is that limited to no knowledge of the structural properties is required. This allows for methods and algorithms that are modular and eliminate the uncertainty around developing a structural model and estimating its parameters.

A mathematical model that is very widely used in SHM and especially under the Statistical Pattern Recognition Paradigm is the Continuous Wavelet Transform (CWT). Research on the application of the CWT for SHM includes the observation of changes in the wavelet coefficients under different loading conditions,[6,7] the extraction of features from the CWT[8–10] and the combination of the CWT with other signal processing methods such as Empirical Mode Decomposition (EMD).[11] The literature on the application of wavelets in the field of SHM is so rich that has spurred the publication of several review papers. Comprehensive reviews on the intersection of the wavelet transform and SHM can be found in Refs. 12, 13, or 14.

An important application of SPR is the structural damage detection. The patterns are used to track the change of the structures and to detect damages. The existing works on the statistical detection of structural damages can be classified into two categories. The first group uses the time-domain information to detect

Further author information: (Send correspondence to Yizheng Liao)
Yizheng Liao: E-mail: yzliao@stanford.edu
Konstantinos Balafas: E-mail: balafas@stanford.edu
Ram Rajagopal: E-mail: ramr@stanford.edu
Anne S. Kiremidjian: E-mail: ask@stanford.edu

Sensors and Smart Structures Technologies for Civil, Mechanical, and Aerospace Systems 2015, edited by Jerome P. Lynch, Kon-Well Wang, Hoon Sohn, Proc. of SPIE Vol. 9435, 94350S
 · doi: 10.1117/12.2084495

damage. For example, the algorithms in Refs. 15 and 16 fit the structural responses with the autoregressive moving average (ARMA) model and then perform hypothesis testing on the model coefficients. Ref. 17 models the ARMA coefficients as a Gaussian mixture. The damage is diagnosed by measuring the distance between the Gaussian mixtures fitted by the undamaged and damaged data. The second group of the structural damage detection algorithms use the frequency-domain information as the damage sensitive features. Examples include Refs. 18, 19 and 20. Our proposed damage detection algorithm is within this group. Ref. 10 uses the wavelet parameters as the damage sensitive features, which are similar to our work. However, it focuses on the change of the frequencies but we use the wavelet coefficients as statistical inferences. Using statistical inferences to detect structural damages allows us to design the algorithm without considering the specific structural models. Refs. 21, 22, and 23 introduces a new set of damage detectors that can make decision in a sequential manner. This new set of detectors minimize the detection delay, which is significant in the damage detection problem. All of these three algorithms use the time domain information as the features. In this paper, we propose a new online damage detector that uses the frequency domain information as the damage sensitive features.

Our first contribution in this paper is formulating the Continuous Wavelet Transform model and proposing the maximum likelihood estimator of the CWT coefficients. This is discussed in Section 2. The second contribution is a sequential structural damage detection algorithm that uses the features from CWT as the statistical inferences. We also discuss how to use the Principal Component Analysis to choose the truly sensitive features and to remove noises. The damage detection algorithm is outlined in Section 3. Section 4 is our third contribution: validating the proposed algorithms with numerical simulations and showing the proposed damage detector is asymptotically optimal. Section 5 concludes the paper.

2. STATISTICAL MODEL FORMULATION

Let $a(t)$ be the acceleration response of the system, where t denotes time. The Continuous Wavelet Transform (CWT) of the signal $a(t)$ will be denoted as $Wa(u,s)$ and is defined as:

$$Wa(u,s) = \int_{-\infty}^{\infty} a(t) \frac{1}{\sqrt{s}} \psi^* \left(\frac{t-u}{s} \right) dt \tag{1}$$

where u refers to shift (a measure of time), s refers to wavelet scale (a measure of frequency) and the $(\cdot)^*$ operator is the complex conjugate. Let $y_t(s)$ be the wavelet coefficients at shift t which will be referred to as wavelet "slice" at time t.

$$y_t(s) = Wa(t,s) \tag{2}$$

Let us define a random process of wavelet scale, $\Psi(s)$, that represents the fundamental shape of the wavelet slices and only depends on the damage state of the structure. The realizations of $\Psi(s)$. at each time t are denoted by $\Psi_t(s)$.

ASSUMPTION 1. *The realizations of $\Psi(s)$ can be written as:*

$$\Psi_t(s) = \overline{\Psi}(s) + \varepsilon_t(s) \tag{3}$$

where $\overline{\Psi}(s)$ is an unobservable function of wavelet scale and its shape only depends on the damage state of the structure.

Define the functional $\mathcal{F}$ for any function f such that:

$$\mathcal{F}(f;a,b,c)(s) = a \cdot f(b \cdot s + c) \tag{4}$$

ASSUMPTION 2. *Each wavelet slice, $y_t(s)$ can be expressed as:*

$$\begin{aligned} y_t(s) &= \mathcal{F}(\Psi;a_t,b_t,c_t)(s) + \Delta y(s) \\ &= a_t \Psi(b_t \cdot s + c_t) + \Delta y(s) \end{aligned} \tag{5}$$

where a_t, b_t and c_t are, generally unobservable, scalar parameters that represent the effect of the input motion on the system's response, such as amplitude and frequency content, and $\Delta y(s)$ is a function of scale that represents effects not captured by the first term.

Null Hypothesis: while the structure is undamaged, the realizations of $\Psi(s)$ are drawn from the same distribution. When damage occurs, the behavior of the structure changes and, thus, the shape of $\bar{\Psi}(s)$ is assumed to change. Since $\bar{\Psi}(s)$ is unobservable, the aforementioned change in shape is manifested as a change in the distribution of $\Psi(s)$.

Combining Equations 3 and 5, we can obtain the following expression for the wavelet coefficients at time t:

$$\begin{aligned} y_t(s) &= a_t \overline{\Psi}(b_t \cdot s + c_t) + a_t \varepsilon_t (b_t \cdot s + c_t) + \Delta y(s) \\ &= \mathcal{F}\left(\overline{\Psi}; a_t, b_t, c_t\right)(s) + \mathcal{F}(\varepsilon_t; a_t, b_t, c_t)(s) + \Delta y(s) \end{aligned} \tag{6}$$

Without loss of generality, we can define the slice at time t_0 as a reference slice. The reference slice will serve as a baseline for the model and, thus, would have to correspond to the undamaged state of the structure. In the present analysis, the reference slice is selected manually so that it is relatively smooth and its general shape is representative of the shape of the majority of the rest of the slices. Equation 5 can be written for the reference slice:

$$\begin{aligned} y_0(s) &= \mathcal{F}(\Psi; a_0, b_0, c_0)(s) + \Delta y(s) \\ &= a_0 \Psi(b_0 \cdot s + c_0) + \Delta y(s) \\ &= a_0 \overline{\Psi}(b_0 \cdot s + c_0) + a_0 \varepsilon_0 (b_0 \cdot s + c_0) + \Delta y(s) \end{aligned} \tag{7}$$

Solving Equation 6 for $\overline{\Psi}(s)$ and substituting in Equation 7, we obtain:

$$\begin{aligned} y_0(s) = &\frac{a_0}{a_t} y_t\left(\frac{b_0}{b_t} s + \frac{c_0 - c_t}{b_t}\right) \\ &- a_0 \varepsilon_t (b_0 s + c_0) - \frac{a_0}{a_t} \Delta y\left(\frac{b_0}{b_t} s + \frac{c_0 - c_t}{b_t}\right) \\ &+ a_0 \varepsilon_0 (b_0 s + c_0) + \Delta y(s) \end{aligned} \tag{8}$$

Define the following:

$$\tilde{a}_t = \frac{a_0}{a_t} \tag{9a}$$

$$\tilde{b}_t = \frac{b_0}{b_t} \tag{9b}$$

$$\tilde{c}_t = \frac{c_0 - c_t}{b_t} \tag{9c}$$

$$\tilde{\varepsilon}_t(s) = a_0 \varepsilon_0 (b_0 s + c_0) - a_0 \varepsilon_t (b_0 s + c_0) \tag{9d}$$

$$\widetilde{\Delta y}(s) = \Delta y(s) - \tilde{a}_t \Delta y\left(\tilde{b}_t s + \tilde{c}_t\right) \tag{9e}$$

Equation 8 then becomes:

$$y_0(s) = \tilde{a}_t y_t\left(\tilde{b}_t s + \tilde{c}_t\right) + \tilde{\varepsilon}_t(s) + \widetilde{\Delta y}(s) \tag{10}$$

The scalar parameters $\tilde{a}_t$, $\tilde{b}_t$ and $\tilde{c}_t$ can be estimated from the data and using the reference slice $y_0(s)$.

In order to obtain an estimate for the transformed error term, $\tilde{\varepsilon}_t(s)$, the wavelet slices can be transformed as follows:

$$y'_t(s) = \tilde{a}_t y_t\left(\tilde{b}_t s + \tilde{c}_t\right) \tag{11}$$

As a result, and since the transformed error term, $\tilde{\varepsilon}_t(s)$ is a zero-mean process, a plug-in estimate for the transformed unmodeled effects (bias) term, $\widetilde{\Delta y}(s)$, can be obtained by:

$$\widehat{\Delta y}(s) = \sum_{t=1}^{t=N} y_0(s) - y_t'(s) \tag{12}$$

An estimate for the transformed noise terms, $\tilde{\varepsilon}_t(s)$ can be obtained as:

$$\hat{\varepsilon}_t(s) = y_0(s) - y_t'(s) - \widehat{\Delta y}(s) \tag{13}$$

The statistical model shown in Equation 6 implies that the input motion has three effects on the "fundamental" shape function, $\overline{\Psi}(s)$: a uniform scaling, a stretch and a shift in the wavelet scale domain. It is, by design, a simple model that captures the intuitive effects of a ground motion on the response of a structure, accounting for the temporally-varied amplitude and frequency content of an earthquake. Even though the function $\overline{\Psi}(s)$ cannot be observed or extracted from the observations, the transformation presented in Equation 11 maps all the wavelet slices to the same reference in terms of signal energy and bandwidth. The transformed error terms, as well as the estimated model parameters, can be used to test whether the slices are indeed drawn from the same distribution. The case where not all slices are drawn from the undamaged distribution implies that damage has occurred in the structure.

2.1 Estimation of the model parameters

The model parameters, namely the parameters defined in Equation 9 plus the transformed noise covariance matrix, will be estimated using Maximum Likelihood Estimation. Specifically, the parameters will be estimated by minimizing the negative log-likelihood function, as shown in Equation 14.

$$\left[\hat{a}, \hat{b}, \hat{c}, \hat{\Delta y}, \hat{\Sigma}\right] = \underset{a,b,c,\Delta y,\Sigma}{\arg\min} -\ell\left(y_0 | y_1, y_2, \ldots, y_N; a, b, c, \Delta y, \Sigma\right) \tag{14}$$

Assumption 3. *The transformed error terms, $\tilde{\varepsilon}_t(s)$, are independent, with respect to the time sample, and identically distributed Gaussian Processes.*

Assumption 3 is very important for the estimation of the model parameters. The assumption of independence simplifies the modeling of the joint likelihood of the different slices. Furthermore, when the slices not to be assumed temporally independent, the model would be biased towards the particular excitation that the data was generated from. Assuming that the error terms are Gaussian Processes also simplifies the solution to the optimization problem posed in Equation 14. Based on Assumption 3, Equation 14 can be written as:

$$\left[\hat{a}, \hat{b}, \hat{c}, \hat{\Delta y}, \hat{\Sigma}\right] = \underset{a,b,c,\Delta y,\Sigma}{\arg\min} \sum_{i=1}^{N} -\ell\left(y_0 | y_i; a_i, b_i, c_i, \Delta y, \Sigma\right) \tag{15}$$

Finally, since the error terms are assumed to be Gaussian, Equation 15 can be further written as:

$$\begin{aligned}\left[\hat{a}, \hat{b}, \hat{c}, \hat{\Delta y}, \hat{\Sigma}\right] = \underset{a,b,c,\Delta y,\Sigma}{\arg\min} \sum_{i=1}^{N} & -\frac{M}{2} - \frac{1}{2}\log\det\Sigma - \\ & - \frac{1}{2}\left(a_i y_i\left(b_i s + c_i\right) - y_0 - \Delta y\right)^T \Sigma^{-1}\left(a_i y_i\left(b_i s + c_i\right) - y_0 - \Delta y\right)\end{aligned} \tag{16}$$

At a proof-of-concept level, the following recursive algorithm was used in the present analysis in order to decouple the terms of the summation in Equation 16 and facilitate the numerical estimation of the parameters:

1. Initialize Δy and $\Sigma_{\tilde{\varepsilon}}$ to an uninformed prior. In the present analysis, $\Delta y^{(0)} = 0$ and $\Sigma_{\tilde{\varepsilon}}^{(0)} = I$, where I is the $M \times M$ identity matrix.

2. For $t = 1 \ldots N$, calculate the parameters $\hat{a}_t^{(k+1)}$, $\hat{b}_t^{(k+1)}$, $\hat{c}_t^{(k+1)}$ using Maximum Likelihood Estimation.

3. Calculate the transformed slices from Equation 11.

4. Calculate the bias term from Equation 12.

5. Calculate the error terms from Equation 13.

6. Estimate the covariance matrix from the error terms.

7. Repeat Steps 2 through 6 until the bias term and covariance matrix converge.

In the outlined algorithm, the superscripts in parentheses refer to each algorithm iteration.

It should be noted that this algorithm need only be applied to a reference signal where the structure is a priori known, or assumed, to be undamaged. Once estimated, the covariance matrix and bias term will refer to the undamaged state of the structure and do not need to be estimated again when the model is applied to a record coming from the same structure but with unknown damage state.

The outlined algorithm requires the estimation and inversion of the covariance matrix of generally high-dimensional random variables. The estimation of the covariance matrix is a well-studied problem and several parametric and non-parametric estimation methods exist in the literature.[24–26] The sample covariance matrix was found to be numerically unstable, especially after a few iterations of the presented algorithm and did not converge. To overcome this problem, a parametric covariance function was fit to the data and its parameters were estimated by maximizing the marginal log-likelihood of the data. In the results presented in subsequent sections, a Matern covariance function was used and the fitting was performed using the Gaussian Processes for Machine Learning (GPML) toolbox, which is based on Ref.27.

3. DAMAGE DETECTION ALGORITHM

A typical damage detection process contains three subcomponents: (i) collecting structural responses; (ii) extracting the damage sensitive features; and (iii) detecting damages via statistical inferences.[28] In this proposed algorithm, the structural responses are sequentially obtained from multiple sensors. In (ii), we estimate the transformed noise terms $\hat{\epsilon}_t(s)$ based on Equation 13 and other relative equations, as we have discussed in previous sections. Unlike the algorithms in Refs. 21 and 28, which use the fitted model coefficients as the damage sensitive features (DSFs) directly, we use Principal Components Analysis (PCA) to select and extract the DSFs. PCA helps to remove the irrelative information and to choose the truly sensitive features. In (iii), the sequential detectors identify the damages in a Bayesian framework.

3.1 Feature Extraction

In the proposed damage detection algorithm, the DSF extraction consists of two steps: (i) estimation of the transformed noise term $\hat{\epsilon}_t(s)$ and (ii) extraction of the principal components. For notation convenience, we will use $x_s(t)$ to denote the estimate of the transformed noise term $\hat{\epsilon}_t(s)$. To find $x_s(t)$, we can apply Equation 11 to Equation 13 and Equation 16.

Let $X(t) \in \mathcal{R}^p$ denote a vector that contains the transformed noise terms of p wavelet scales at time t, i.e. $X(t) = [x_1(t), x_2(t), \ldots, x_p(t)]^T$. In many cases, only a subset of the p wavelet scales are sensitive to the damages. The insensitive wavelet scales are irrelative to the damage detection and may weaken the detection performance. Therefore, we should only use these scales that are sensitive to the damages as our DSFs. In this detection algorithm, we use PCA to find these damage sensitive wavelet scales. PCA uses a small number of dimensions that are sensitive to damage to represent the n observations in p dimensional space. Each of the dimensions found by PCA is a linear combination of the transformed noise terms of p wavelet scales. PCA helps to reduce the noise of the data and to capture the most sensitive wavelet scales.

The first principal component is the linear combination of the noises of wavelet scales

$$z_1(t) = \phi_{11}x_1(t) + \phi_{21}x_2(t) + \cdots + \phi_{p1}x_p(t) = \phi_1^T X(t) \tag{17}$$

where $z_1(t)$ is the first principal component at time t and $\phi_{11}, \ldots, \phi_{p1}$ are the *loadings* of the first principal component. We use $\phi_1 = (\phi_{11}, \ldots, \phi_{p1})^T$ to denote the loading vector of the first principal component. The loadings have to satisfy that

$$\sum_{i=1}^{p} \phi_{i1}^2 = 1. \tag{18}$$

Equation 17 projects a p-dimensional data set to a single value. As discussed in Ref. 29, the first principal component captures the largest variance of the original data set. To find the first principal component loading vector, we have to solve the following optimization problem over n observations:

$$\max_{\phi_{11},\ldots,\phi_{p1}} \left\{ \frac{1}{n} \sum_{t=1}^{n} \left(\sum_{k=1}^{p} \phi_{k1} x_k(t) \right)^2 \right\} \quad \text{subject to} \sum_{k=1}^{p} \phi_{k1}^2 = 1. \tag{19}$$

There are rich literatures on how to solve the optimization problem above and several well-known algorithms are discussed by Refs. 29 and 30.

After finding the first principal component $z_1(t)$, we can find the second principal component that captures the largest variances that are uncorrelated with $z_1(t)$. The second principal component is also a linear combination of the transformed noises and has the form as

$$z_2(t) = \phi_{12} x_1(t) + \phi_{22} x_2(t) + \cdots + \phi_{p2} x_p(t) = \phi_2^T X(t) \tag{20}$$

where ϕ_2 is the loading vector of the second principal component and satisfies the same constraint in Equation 18. In addition, since $z_2(t)$ is uncorrelated with $z_1(t)$, ϕ_2 has to be orthogonal to ϕ_1, i.e. $\phi_1^T \phi_2 = 0$. The second principal component can be found with the same method as the first principal component. We can continue the process above to find p principal components. As discussed in Ref. 29, the variance explained by each principal component is monotonically decreasing. It means that the first principal component captures the largest variance. The second principal component explains the largest variance among the rest principal components and so on. Many works have shown that the first several principal components can explain most variances of the original data set.[29,31] Therefore, rather than using the p-dimensional transformed noise as the DSF for damage detection, we only need to use q principal components as the DSF, where q is less than p. In Section 4, we will discuss how to pick up the number q.

3.2 Damage Detection

Our primary interest in damage detection problem is estimating the damage time. Assume that the damage occurs at a random time λ with a prior distribution $\pi(\lambda)$. Our goal is to detect this damage as quickly as possible.

Because of Assumption 3, we can assume that $X(t)$ is independently and identically distributed (i.i.d) with a multivariate Gaussian distribution with mean $\mu_p \in \mathcal{R}^p$ and covariance matrix $\Sigma_p \in \mathcal{R}^{p \times p}$. As discussed in previous section, each principal component is a linear combination of the elements of $X(t)$. Therefore, z_i follows a single-variant Gaussian distribution with mean $\mu_i = \phi_i^T \mu_p$ and variance $\sigma_i^2 = \phi_i^T \Sigma_p \phi_i$. Let $Z(t)$ denote the vector that contains q principal components as the DSF, i.e. $Z(t) = [z_1(t), \ldots, z_q(t)]$. Then $Z(t)$ is i.i.d with a multivariate Gaussian distribution, which is shown below:

$$Z(t) \sim \mathcal{N}(\mu_z, \Sigma_z), \tag{21}$$

$$\mu_z = [\phi_1^T \mu_p, \ldots, \phi_q^T \mu_p]^T, \tag{22}$$

$$\Sigma_z = \begin{pmatrix} \phi_1^T \Sigma_p \phi_1 & 0 & \ldots & 0 \\ 0 & \phi_2^T \Sigma_p \phi_2 & \ldots & 0 \\ \vdots & \vdots & \vdots & \vdots \\ 0 & 0 & \ldots & \phi_q^T \Sigma_p \phi_q \end{pmatrix}. \tag{23}$$

The covariance matrix Σ_d is diagonal based on the fact that the principal components are uncorrelated with each other.

ASSUMPTION 4. *$X(t)$ is i.i.d with density g when $t < \lambda$ and is i.i.d with density f when $t \geq \lambda$.*

Both densities are obtained prior to the analysis from simulations or experiments. Since we use $Z(t)$ as the DSF, Assumption 4 is equivalently states that $Z(t)$ is i.i.d with a Gaussian distribution g_z when $t < \lambda$ and is i.i.d with the other Gaussian distribution f_z when $t \geq \lambda$. Both distributions can be estimated based on the data of $Z(t)$ empirically or transformed from the distributions of $X(t)$.

Since our primary interest is detecting the damages, therefore, we apply compute the loading vectors based on the damaged data set. A standard step before applying PCA is subtracting the means such that the data is zero-mean. This step helps to avoid the case that different features have different magnitude. In our case, the post-damaged distribution will be zero-mean, i.e $\mu_f = [0, 0, \ldots, 0]^T$. In addition, the undamaged distribution will have non-zero mean since the undamaged data are subtracted by the post-damaged mean as well. This does not contradict with Assumption 3. In Assumption 3, we assume that $X(t)$ has zero mean in undamaged status. After PCA projection, $Z(t)$ does not have zero mean since we subtract the post-damaged mean from $X(t)$. The loading vectors should be only computed once and then can be used directly. For every new observation, before linear projection, we should subtract the post-damaged mean as well.

A sequence of DSFs up to the time n can be represented as $\mathbf{Z}^n = (Z(1), Z(2), \ldots, Z(n))$. In the Bayesian formulation, the joint distribution of λ and $\mathbf{Z}^n$ is

$$P(\lambda, \mathbf{Z}^n) = \pi(\lambda) P(\mathbf{Z}^n | \lambda). \tag{24}$$

If the damage occurs at time $\lambda = k$, based on our discussion above, we can assume $Z(1), \ldots, Z(k-1)$ is i.i.d with the Gaussian density g_z and $Z(k), \ldots, Z(n)$ is i.i.d with the Gaussian density f_z. Therefore, the likelihood function is

$$P(\mathbf{Z}^n | \lambda = k) = \prod_{t=1}^{k-1} g_z(Z(t)) \prod_{t=k}^{n} f_z(Z(t)). \tag{25}$$

The posterior probability can be computed as

$$\begin{aligned} \gamma^n(k) := P(\lambda = k | \mathbf{Z}^n) &= \frac{P(\lambda = k, \mathbf{Z}^n)}{P(\mathbf{Z}^n)} \\ &= \frac{\pi(\lambda = k) P(\mathbf{Z}^n | \lambda = k)}{P(\mathbf{Z}^n)} \\ &\propto \pi(\lambda = k) P(\mathbf{Z}^n | \lambda = k) \end{aligned}$$

A detection problem has two constraints: the probability of false alarm, which is defined as

$$\alpha = P(\tau < \lambda),$$

where τ is the estimate of the damage time, and the detection delay, which is defined as

$$d = E(\tau - \lambda | \tau \geq \lambda).$$

As discussed in Refs. 28 and 32, given a desired probability of false alarm α, the following detector minimizes the detection delay d,

$$\tau = \inf\{n : P(\lambda \leq n | \mathbf{Z}^n) \geq 1 - \alpha\}, \tag{26}$$

In our setup, given the most allowable false alarm rate α, we can declare damage and find the damage time when $\sum_{k=1}^{n} \gamma^n(k)$ is larger than $1 - \alpha$ at its first time.

Now we propose our sequential damage detection algorithm at each time n as follow:

1. Acquire the structural signal $a(n)$.

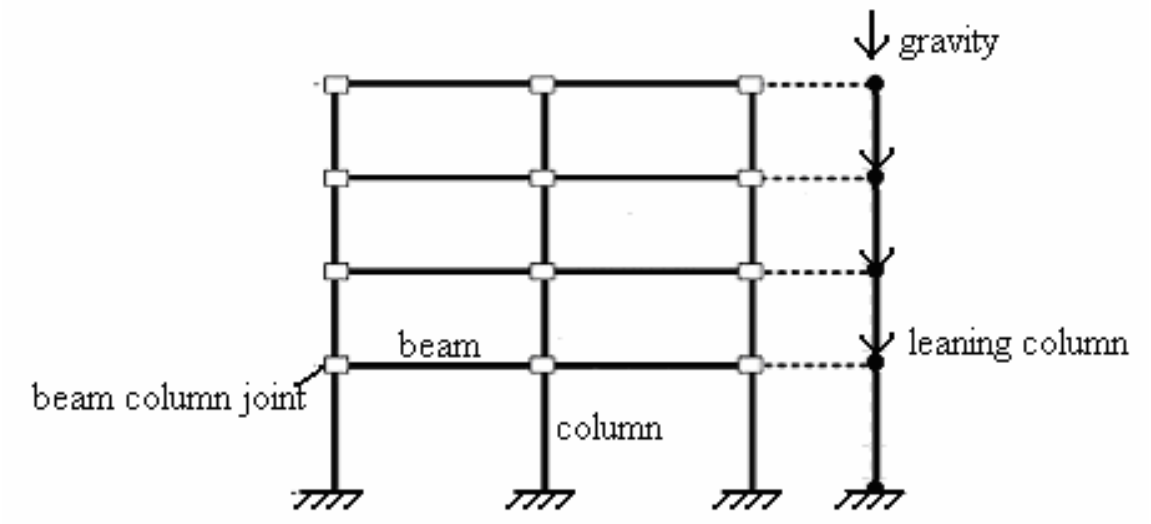

Figure 1: Schematic of the four-story steel moment frame used for the simulations. Figure reprinted from 35

2. Perform wavelet transformation and estimate the model parameters via the the maximum likelihood method presented in Section 2.1.
3. Compute the transformed noise term $x_s(n)$ over all the wavelet scales.
4. Compute the DSF vector $Z(n)$ by subtracting the post-damaged mean from the transformed noise vector $X(n)$ and then projecting the results to the principal component directions. The loading vectors ϕ_i are pre-computed based on the experiments and simulations.
5. Compute the prior probability $\pi(k)$ for $1 \leq k \leq n+1$, where $\pi(n+1) = \sum_{k=n+1}^{\infty} \pi(k) = 1 - \sum_{k=1}^{n} \pi(k)$.
6. Compute the likelihood for $1 \leq k \leq n+1$ based on Equation 25.
7. Compute $\gamma^n(k) = \pi(\lambda = k) P(\mathbf{Z}^n | \lambda = k)$ for $1 \leq k \leq n+1$. Then normalize $\gamma^n(k)$ such that $\sum_{k=1}^{n+1} \gamma^n(k) = 1$.
8. Declare the damage time estimate $\tau = n$ when $\sum_{k=1}^{n} \gamma^n(k) \geq 1 - \alpha$ at the first time.

4. NUMERICAL RESULTS

In this section, we validate the proposed algorithms for estimating wavelet coefficients and detecting structural damages by using the structural responses from a four story structure. We explore how the detection delay changes with different false alarm rates. In addition, we investigate how the number of principal components affects the performance of the damage detection.

4.1 Description of Simulation

The algorithms described are applied to a simulated dataset of acceleration responses due to earthquake excitation. The structure considered is a four-story steel moment-frame originally designed and tested by Lignos *et al.*,[33] as shown in Fig. 1. A Finite Element Model was developed and calibrated in OpenSees[34] by the original researchers. The Finite Element Model was subjected to a series of earthquakes under varied intensities and the acceleration response at each floor was captured. The presence of damage was quantified by the moment-rotation behavior at pre-defined "plastic-hinge" locations at the beams and columns of each story. A purely linear relationship between moment and rotation indicates no damage and the presence of damage anywhere within a story was taken to denote damage in the story.

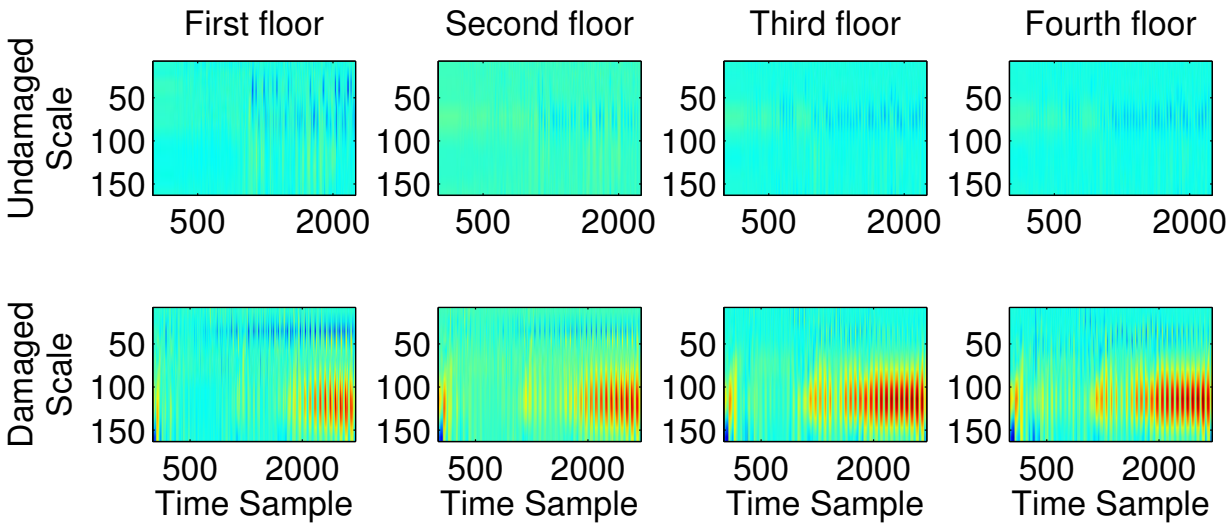

Figure 2: Transformed residuals for all floors in the undamaged (top row) and damaged (bottom row) state

The wavelet coefficients of the acceleration response at each floor are calculated using the Morlet wavelet. The transformed residuals are calculated according to the previously described algorithm. The parameters of the wavelet transform are estimated over $p = 150$ wavelet scales. Figure 2 shows the transformed residuals in each floor for the undamaged and damaged state. It can be observed that in the undamaged state the residuals are uniform over time and close to zero, while in the damaged state the distribution changes.

The damages are introduced to each floor independently. The damage time λ follows a geometric distribution with the parameter $\rho = 0.1$, i.e. $\lambda \sim Geo(0.1)$. The structural responses $a(t)$ are recorded from each floor independently and simultaneously. In our simulation, we regard each floor as an independent object and discard the correlation among floors.

4.2 Results and Discussion

The loading vectors of PCA are computed by the singular value decomposition algorithm. The number of principle components is decided by the proportion of variance explained (PVE) by each principle component. The PVE of the ith principle component is given by

$$PVE = \frac{\sum_{t=1}^{n} \left(\sum_{j=1}^{p} \phi_{jt} x_j(t) \right)^2}{\sum_{j=1}^{p} \sum_{t=1}^{n} x_j^2(t)}. \tag{27}$$

Fig. 3 shows the PVE explained by the first ten principle components for ten different strong motions. The first principle component captures around 45% of the variance and the first three principle components explain about 90% variance.

Fig. 4 shows the expected delay against the false alarm rate from 0.5 to 10^{-15} over 300 iterations. As expected, the algorithm detects the damage faster when the false alarm rate is larger. When α is reduced, the expected detection delay increases. In addition, we can observe that the detector that uses 7 principal components has the smallest detection delay in general. The reason of this behavior is that the cumulative variances are largest. It means that more information can reduce the detection delay.

Ref. 32 proves that the optimal delay is

$$E[\tau - \lambda | \tau \geq \lambda] = \frac{|\log \alpha|}{-\log(1-\rho) + I} \tag{28}$$

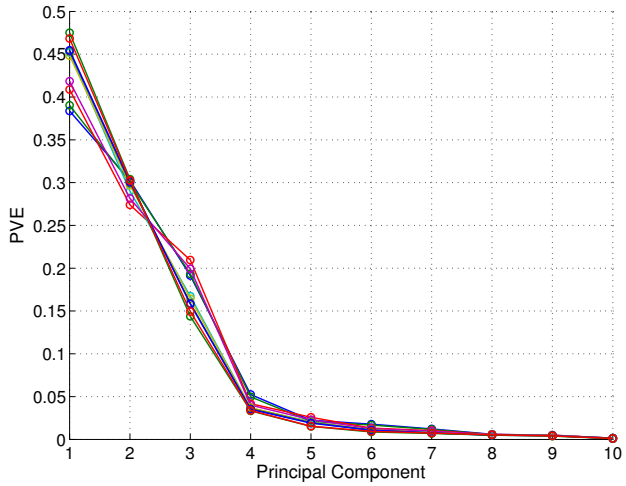

(a) The proportion of variance explained by the first ten principle components

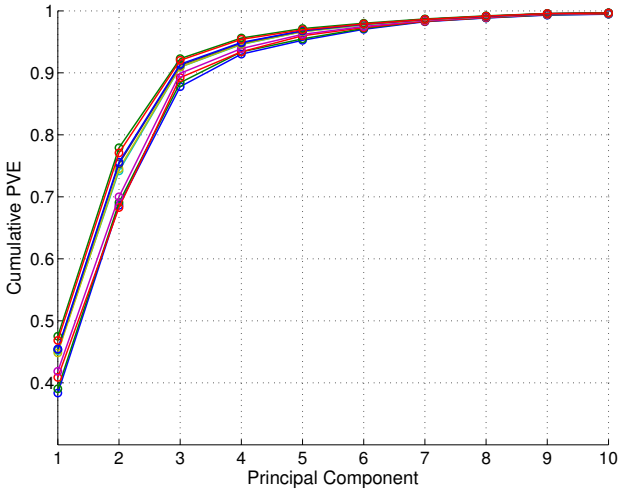

(b) The cumulative proportion of variance explained by the first ten princple components

Figure 3: The proportion of variance explained by the principle components

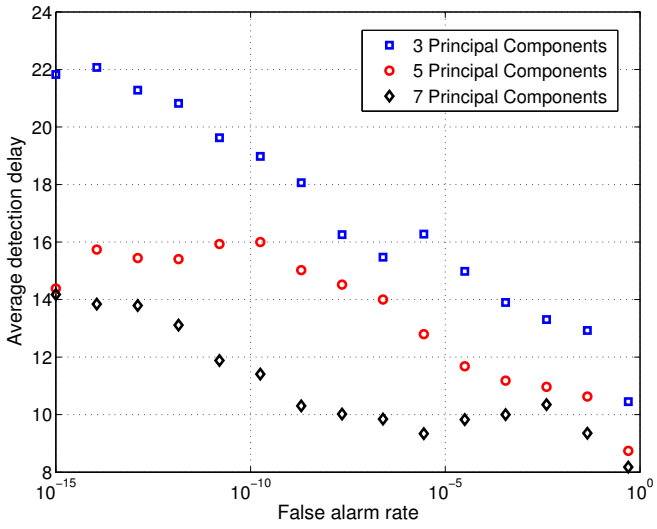

Figure 4: Plots of the expected delay against the false alarm rate

where ρ is the parameter of the geometric prior and I is the Kullback Leibler (KL) divergence, which is defined as

$$I = \int f_z(x) \log \frac{f_z(x)}{g_z(x)} dx. \tag{29}$$

In our problem, both densities g_z and f_z are multivariate Gaussian distributions. Therefore, the KL divergence becomes to

$$I = \frac{1}{2}\left(tr(\Sigma_f^{-1}\Sigma_g) + (\mu_f - \mu_g)^T \Sigma_f^{-1}(\mu_f - \mu_g) - k + \log\left(\frac{det\Sigma_f}{det\Sigma_g}\right)\right), \tag{30}$$

where μ_g and Σ_g are the mean and the covariance matrix followed by the density g_z, μ_f and Σ_f are the mean and the covariance matrix followed by the density f_z, and k is the dimension of the distributions.

In our simulation, the means and covariance matrices are estimated empirically from the simulation. We compute the KL divergences according to Equation 30 and their values are shown in Table. 1. From Table. 1, we

Number of Principal Component	KL divergence (I)
3	1.5633
5	2.2023
7	2.4045

Table 1: KL divergence of each number of principal component

can see that when more principal components are used as the DSF, the KL divergence is larger. It means that the distributions before and after damage are more different. Based on Equation 30, we can also find out that, when more principal components are used as the DSF, the expected detection delay is smaller. This observation is consistent with what we found in Fig. 4.

Fig. 5 plots the expected delay divided by $-\log\alpha$ as a function of $-\log\alpha$ for α from 0.5 to 10^{-15}. The dash line is the asymptotical limit. We can observe that as $\alpha \to 0$, the expected delay coverages to the asymptotical limit. It shows that our proposed detector is asymptotically optimal, which is consistent with the results in Refs. 28 and 32. This figure also shows a consistent result that the detector that uses more principal components as the DSF has better performance.

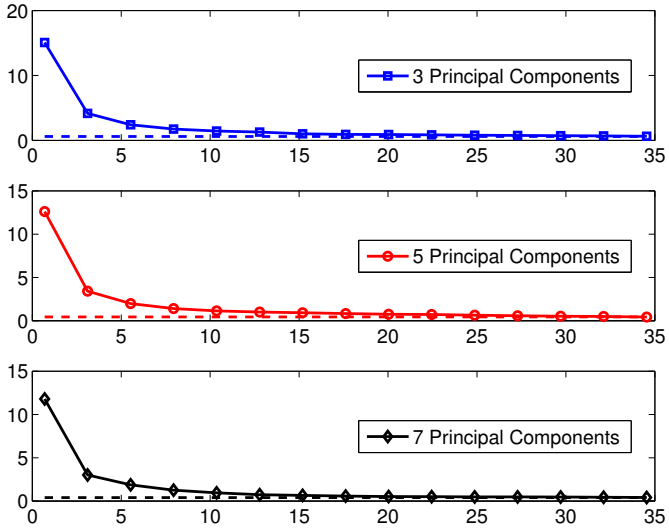

Figure 5: Plots of the slope $\frac{1}{-\log\alpha} E[\tau - \lambda | \tau \geq \lambda]$ against $-\log\alpha$. The dash line is the asymptotical limit.

5. CONCLUSION

In this paper, we have formulated the continuous wavelet transform model and developed an algorithm to estimate the CWT coefficients. This algorithm computes the CWT coefficients from the structural responses without knowing the information of structures. In addition, we have proposed a damage detection algorithm that uses the CWT noise terms as the statistical inferences. Unlike many other algorithms that use the features from the frequency-based model directly, we have used PCA to select and extract the features that are most sensitive to the damage. As a sequential detector, it continuously takes new principal components as the DSF and reports decisions.

The proposed algorithms have been validated by the simulation data. The results showed that the proposed detector had the minimum detection delay for a given probability of false alarm. In addition, the detector was asymptotically optimal as it converged to an asymptotical bound when the false alarm trends to zero. Also, we discovered that when more principal components were used as the DSF, the expected detection delay was reduced.

ACKNOWLEDGMENTS

The authors would like to thank the National Science Foundation, the George E. Brown Jr. Network for Earthquake Engineering Simulation and the Stanford Graduate Fellowship program for their funding and support of this research through NEESR Grant No. 105651 and the Arvanitidis Fellowship in Memory of William K. Linvill, respectively. They would also like to thank Dimitrios Lignos of McGill University and Laura Eads of Ris for their help, collaboration and data sharing.

REFERENCES

[1] Farrar, C. R. and Sohn, H., "Pattern recognition for structural health monitoring," in [*Workshop on Mitigation of Earthquake Disaster by Advanced Technologies, Las Vegas, NV, USA*], (2000).

[2] Sohn, H., Farrar, C. R., Hunter, N. F., and Worden, K., "Structural health monitoring using statistical pattern recognition techniques," *Journal of Dynamic Systems, Measurement and Control* **123**, 706–711 (February 2001).

[3] Sohn, H. and Farrar, C. R., "Damage diagnosis using time series analysis of vibration signals," *Smart Materials and Structures* **10**(3), 446 (2001).

[4] Fugate, M. L., Sohn, H., and Farrar, C. R., "Unsupervised learning methods for vibration-based damage detection," (2000).

[5] Farrar, C. R. and Worden, K., "An introduction to structural health monitoring," *Philosophical Transactions of the Royal Society A* **365**, 623–632 (2007).

[6] Melhem, H. and Kim, H., "Damage detection in concrete by Fourier and wavelet analyses," *Journal of Engineering Mechanics* **129**, 571–577 (May 2003).

[7] Kim, H. and Melhem, H., "Damage detection of structures by wavelet analysis," *Engineering Structures* **26**, 347–362 (February 2004).

[8] Sun, Q. and Tang, Y., "Singularity analysis using continuous wavelet transform for bearing fault diagnosis," *Mechanical Systems and Signal Processing* **16**, 1025–1041 (November 2002).

[9] Robertson, A. N., Farrar, C. R., and Sohn, H., "Singularity detection for structural health monitoring using holder exponents," in [*Proc. SPIE 5057, Smart Structures and Materials: Smart Systems and Nondestructive Evaluation for Civil Infrastructures, 569*], (2003).

[10] Noh, H. Y., Nair, K. K., Lignos, D., and Kiremidjian, A. S., "Use of wavelet-based damage-sensitive features for structural damage diagnosis using strong motion data," *Journal of Structural Engineering* **137**, 1215–1228 (October 2011).

[11] Li, H., Deng, X., and Dai, H., "Structural damage detection using the combination method of EMD and wavelet analysis," *Mechanical Systems and Signal Processing* **21**, 298–306 (January 2007).

[12] Peng, Z. K. and Chu, F. L., "Application of the wavelet transform in machine condition monitoring and fault diagnostics: a review with bibliography," *Mechanical Systems and Signal Processing* **18**, 199–221 (March 2004).

[13] Taha, M. M. R., Noureldin, A., Lucero, J. L., and Baca, T. J., "Wavelet transform for structural health monitoring: a compendium of uses and features," *Structural Health Monitoring* **5**, 267–295 (September 2006).

[14] Staszewski, W. J. and Robertson, A. N., "Time-frequency and time-scale analyses for structural health monitoring," *Philosophical Transactions of the Royal Society A* **365**, 449–477 (February 2007).

[15] Nair, K. K., Kiremidjian, A. S., and Law, K. H., "Time series-based damage detection and localization algorithm with application to the asce benchmark structure," *Journal of Sound and Vibration* **291**(1), 349–368 (2006).

[16] Noh, H. Y., Nair, K. K., Kiremidjian, A. S., and Loh, C., "Application of time series based damage detection algorithms to the benchmark experiment at the national center for research on earthquake engineering (ncree) in taipei, taiwan," *Smart Structures and Systems* **5**(1), 95–117 (2009).

[17] Nair, K. K. and Kiremidjian, A. S., "Time series based structural damage detection algorithm using gaussian mixtures modeling," *Journal of Dynamic Systems, Measurement, and Control* **129**(3), 285–293 (2007).

[18] Salawu, O., "Detection of structural damage through changes in frequency: a review," *Engineering structures* **19**(9), 718–723 (1997).

[19] Hou, Z., Noori, M., and Amand, R. S., "Wavelet-based approach for structural damage detection," *Journal of Engineering mechanics* **126**(7), 677–683 (2000).

[20] Hackmann, G., Guo, W., Yan, G., Sun, Z., Lu, C., and Dyke, S., "Cyber-physical codesign of distributed structural health monitoring with wireless sensor networks," *Parallel and Distributed Systems, IEEE Transactions on* **25**(1), 63–72 (2014).

[21] Noh, H., Rajagopal, R., and Kiremidjian, A., "Damage diagnosis algorithm for civil structures using a sequential change point detection method and time-series analysis," in [*Proceedings of the 8th International Workshop on Structural Health Monitoring*], 55–62 (2011).

[22] Mollineaux, M. and Rajagopal, R., "Sequential detection of progressive damage," in [*SPIE Smart Structures and Materials+ Nondestructive Evaluation and Health Monitoring*], 86920U–86920U, International Society for Optics and Photonics (2013).

[23] Liao, Y., Mollineaux, M., Hsu, R., Bartlett, R., Singla, A., Raja, A., Bajwa, R., and Rajagopal, R., "Snowfort: An open source wireless sensor network for data analytics in infrastructure and environmental monitoring," *Sensors Journal, IEEE* **14**, 4253–4263 (Dec 2014).

[24] Anderson, T. W., "Asymptotically efficient estimation of covariance matrices with linear structure," *The Annals of Statistics* **1**, 135–141 (January 1973).

[25] Andrews, D. W. K., "Heteroskedasticity and autocorrelation consistent covariance matrix estimation," *Econometrica* **59**, 817–858 (May 1991).

[26] Chen, Y., Wiesel, A., Eldar, Y. C., and Hero, A., "Shrinkage algorithms for MMSE covariance estimation," *IEEE Transactions on Signal Processing* **58**, 5016–5029 (October 2010).

[27] Rasmussen, C. E. and Williams, C. K. I., [*Gaussian Processes for Machine Learning*], The MIT Press (2006).

[28] Liao, Y. and Rajagopal, R., "Message-passing sequential detection of multiple structural damages," in [*Submitted to 12th International Conference on Applications of Statistics and Probability in Civil Engineering*], (2015).

[29] James, G., Witten, D., Hastie, T., and Tibshirani, R., [*An introduction to statistical learning*], Springer (2013).

[30] Hastie, T., Tibshirani, R., Friedman, J., Hastie, T., Friedman, J., and Tibshirani, R., [*The elements of statistical learning*], Springer (2009).

[31] Zang, C. and Imregun, M., "Structural damage detection using artificial neural networks and measured frf data reduced via principal component projection," *Journal of Sound and Vibration* **242**(5), 813–827 (2001).

[32] Amini, A. A. and Nguyen, X., "Sequential detection of multiple change points in networks: a graphical model approach," *, IEEE Transactions on Information Theory* .

[33] Lignos, D. G., Krawinkler, H., and Whittaker, A. S., "Prediction and validation of sidesway collapse of two scale models of a 4-story steel moment frame," *Earthquake Engineering and Structural Dynamics* **40**, 807–825 (June 2011).

[34] Mazzoni, S., McKenna, F., Scott, M. H., and Fenves, G. L., "Open system for earthquake engineering simulation user command-language manual," tech. rep., Pacific Earthquake Engineering Research Center (May 2009).
[35] Lignos, D., *Sidesway Collapse of Deteriorating Structural Systems Under Seismic Excitations*, PhD thesis, Stanford University (2008).